Proceedings of the Estonian Academy of Sciences,
2019, **68**, 3, 264–275
https://doi.org/10.3176/proc.2019.3.03
Available online at www.eap.ee/proceedings

COMMUNICATIONS
TECHNOLOGY

Multi-source in DF cooperative networks with the PSR protocol based full-duplex energy harvesting over a Rayleigh fading channel: performance analysis

Tan N. Nguyen[a,b], Minh Tran[c*], Duy-Hung Ha[b,d], Tran Thanh Trang[e], and Miroslav Voznak[b]

[a] Wireless Communications Research Group, Faculty of Electrical and Electronics Engineering, Ton Duc Thang University, Ho Chi Minh City, Vietnam
[b] VSB-Technical University of Ostrava, 708 33 Ostrava - Poruba, Czech Republic
[c] Optoelectronics Research Group, Faculty of Electrical and Electronics Engineering, Ton Duc Thang University, Ho Chi Minh City, Vietnam
[d] Faculty of Electrical and Electronics Engineering, Ton Duc Thang University, Ho Chi Minh City, Vietnam
[e] Faculty of Engineering and Technology, Van Hien University, 665-667-669 Dien Bien Phu, Ho Chi Minh City, Vietnam

Received 11 October 2018, accepted 8 January 2019, available online 27 May 2019

Abstract. Due to the tremendous energy consumption growth with ever-increasing connected devices, alternative wireless information and power transfer techniques are important not only for theoretical research but also for saving operational costs and for a sustainable growth of wireless communications. In this paper, we investigate the multi-source in decode-and-forward cooperative networks with the power splitting protocol based full-duplex energy harvesting relaying network over a Rayleigh fading channel. In this system model, the multi-source and the destination communicate with each other by both the direct link and an intermediate helping relay. First, we investigate source selection for the best system performance. Then, the closed-form expression of the outage probability and the symbol error ratio are derived. Finally, the Monte Carlo simulation is used for validating the analytical expressions in connection with all main possible system parameters. The research results show that the analytical and simulation results matched well with each other.

Key words: full-duplex, throughput, outage probability, wireless energy harvesting.

1. INTRODUCTION

Because of the tremendous energy consumption growth with ever-increasing connected devices, alternative wireless information and power transfer techniques are important not only for theoretical research but also for saving operational costs and for a sustainable growth of wireless communications. In this regard, radio frequency (RF) energy harvesting (EH) for a wireless communications system presents a new paradigm that allows wireless nodes to recharge their batteries from the RF signals instead of fixed power grids and the traditional energy sources. In this approach, the RF energy is harvested from ambient electromagnetic

* Corresponding author, tranhoangquangminh@tdtu.edu.vn

sources or from the sources that directionally transmit RF energy for EH purposes [1–7]. Furthermore, RF EH, considered as one of the promising techniques, has received much attention as it can provide unlimited power to the sensor nodes that scavenge energy from the environment (i.e. solar, wind, etc.). Among these, RF energy radiated by ambient transmitters is almost ubiquitous, which can be harvested more effectively from wireless RF signals. Since RF signals can carry energy and information simultaneously, EH and simultaneous wireless information and power transfer (SWIPT) are becoming a more and more promising research direction [8–10]. With the recent advance of RF EH, wireless powered communication networks (WPCNs) have become a new wireless networking technology, where wireless devices (WDs) can be remotely powered by RF wireless energy transfer (WET). Devices in a WPCN are charged by a dedicated wireless energy source [8–10]. In addition, the energy released by the energy source is adjustable to satisfy different physical conditions and service criteria [8,11,12]. Bhatnagar [10] investigated the incorporation of cooperative multiple-input and multiple-output (MIMO) two-way relay systems, where a full-duplex (FD) amplify-and-forward (AF) relay was equipped with multiple antennas. The work in [13] was extended in [14], where the achievable sum rate of a cooperative system with FD MIMO AF relaying was maximized. Cooperative relay networks were studied in [15]. Here, a relay harvests energy from the RF signals broadcast by a source and then utilizes it to assist in the information transfer from the source to its final destination.

In our current work, we investigate the multi-source in decode-and-forward (DF) cooperative networks with the power splitting (PSR) protocol based FD energy harvesting relaying network over a Rayleigh fading channel. In this system model, the multi-source and the destination communicate with each other by both the direct link and an intermediate helping relay. First, we investigate the source selection for the best system performance. Then, the closed-form expression of the outage probability and the symbol error ratio (SER) are derived. Finally, the Monte Carlo simulation is used for validating the analytical expressions in connection with all main possible system parameters. The research results show that the analytical and simulation results matched well with each other. The main contributions of this paper are as follows:

- The source selection for improving the system performance of the multi-source in DF cooperative networks with the PSR protocol based FD energy harvesting relaying network over a Rayleigh fading channel is presented and investigated.
- The closed-form expression of the outage probability and the SER for the proposed system is derived.
- The Monte Carlo simulation is used for validating the analytical expressions in connection with all main possible system parameters.

The rest of this paper is organized as follows. Section 2 describes the system model and the EH protocol used in this paper. Section 3 provides a detailed performance analysis of the system, including exact analysis and asymptotic analysis. The numerical results to validate the analysis are presented in Section 4. Finally, conclusions are drawn in Section 5.

2. SYSTEM MODEL

Figure 1 plots the system model with multi-source (S_n), one relay (R), and one destination (D). The transmission model follows the principles of analog network coding, and this concept is the extension of linear network coding to multihop wireless networks. In our model, every terminal operates in an FD mode and the relay works in a DF mode. The multi-source and destination nodes communicate by two links: one direct link between the multi-source and the destination and one link with the help of the intermediate relay.

In this system model, we denote the channel gain between the node S_n and the relay R as h_{RnD}, between the relay R and the destinations D as h_{RD}, and the direct link between the multi-source and D is h_{S_nD}. Moreover, the interference at R is h_{RR}. All the channels are assumed to be Rayleigh fading channels. Furthermore, the relay has energy only to serve their purpose, so it needs to harvest energy from the node before forwarding the information messages to the destination. The energy harvesting and information processing for this proposed model system are presented in Fig. 2. In this protocol, the transmission is

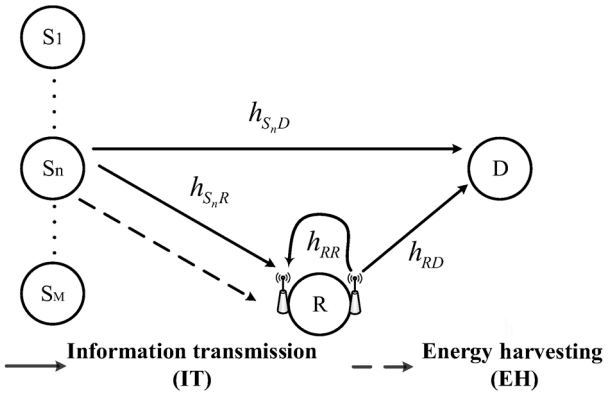

Fig. 1. System model.

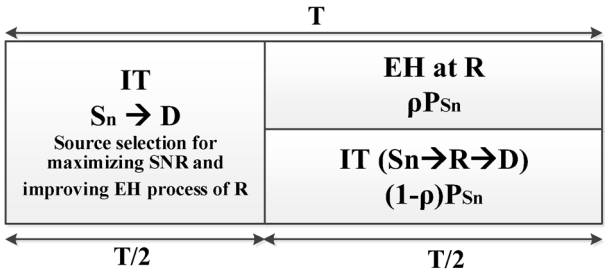

Fig. 2. Energy harvesting and information processing by the adaptive relaying protocol.

divided into blocks of length *T*. Each transmission block consists of two time slots. In the first half-time slot *T*/2, the multi-source S_n transfers the information to the destination by the direct link between the source and the destination. In the remaining half-interval time slot *T*/2, the multi-source transfers information to the destination with the helping relay R. In this remaining interval time, the energy harvesting from the multi-source at the relay node R is ρP_{S_n}, and the relay R transfers the information to the destination with the remaining power $(1-\rho)P_{S_n}$. Finally, the information transformation from the multi-source to the destination is accomplished by both the direct link and the helping relay R [16,17].

3. SYSTEM PERFORMANCE

Suppose the source S_n is chosen to send its information and energy. During the second time slot, S_n sends the normalized signal x_{s_n} to the relay R and destination D with the transmit power P_{S_n}. In the second time slot, the received signals at R and D are, respectively, given by equations (1) and (2):

$$y_r = \sqrt{1-\rho}\,h_{S_nR}x_{s_n} + h_{RR}x_r + n_r, \tag{1}$$

where $\mathrm{E}\left\{\left|x_s\right|^2\right\} = P_s$, $\mathrm{E}\left\{\left|x_r\right|^2\right\} = P_r$ and $\mathrm{E}\{\bullet\}$ is the expectation operator with $n \in (1,2,...,M)$, h_{RR} is the loopback interference channel, n_r is the additive white Gaussian noise (AWGN) with variance N_0;

$$y_d^1 = h_{RD}x_r + n_d^1, \tag{2}$$

where h_{RD} is the relay to destination channel gain and n_d^1 is the AWGN with variance N_0.

In the first time slot, S_n will transmit the data to the destination directly; the received signal destination can be given as

$$y_d^2 = h_{S_nD}x_{S_n} + n_d^2, \tag{3}$$

where h_{S_nD} is the source S_n to the destination channel gain and n_d^2 is the AWGN with variance N_0.

In the second interval, the average transmitted power at the relay can be calculated as

$$P_r = \frac{E_r}{T/2} = \eta\rho P_{S_n}\left|h_{S_nR}\right|^2, \tag{4}$$

where $0 < \eta \le 1$ is the energy conversion efficiency, $0 \le \rho < 1$ is the power splitting factor, P_{S_n} is the transmitted power at source S_n, h_{S_nR} is the source S_n to the relay channel gain.

In this model, we consider the DF protocol. From (1), the signal to noise ratio (SNR) at the relay can be calculated as follows:

$$\gamma_1 = \frac{(1-\rho)\left|h_{S_nR}\right|^2 P_{s_n}}{\left|h_{RR}\right|^2 P_r + N_0}. \tag{5}$$

Substituting (4) into (5) and using the fact that $N_0 << P_s$, (5) can be reformulated as

$$\gamma_1 = \frac{(1-\rho)\left|h_{S_nR}\right|^2 P_{s_n}}{\eta\rho P_{S_n}\left|h_{S_nR}\right|^2\left|h_{RR}\right|^2 + N_0} \approx \frac{(1-\rho)}{\eta\rho\left|h_{RR}\right|^2}. \tag{6}$$

From (2) and (4), the SNR at the destination in the second time slot can be calculated as

$$\gamma_2 = \frac{P_r\left|h_{RD}\right|^2}{N_0} = \frac{\eta\rho P_{S_n}\left|h_{S_nR}\right|^2\left|h_{RD}\right|^2}{N_0}. \tag{7}$$

From (3), the SNR at the destination in the first time slot can be obtained as

$$\gamma_3 = \frac{P_{S_n}\left|h_{S_nD}\right|^2}{N_0}. \tag{8}$$

After the selection combining (SC) receiver, the received SNR at D with DF relaying is given by the following equation:

$$\gamma_{e2e} = \max\left[\min\left(\gamma_1,\gamma_2\right),\gamma_3\right]. \tag{9}$$

Please note that all of the channels belong to Rayleigh fading channels in this system model.

Source selection

From (9), the best source S_{n^*} could be selected to maximize the received SNR at the destination to optimize the transmission performance as follows:

$$n^* = \arg\max_{1\le n\le M}\ \max\left[\min\left(\gamma_1,\gamma_2\right),\gamma_3\right]. \tag{10}$$

We propose the optimal source selection protocol in which the best selection source is selected as follows:

$$\omega_1 = \max_{n=1,2,\ldots,M}\left(\left|h_{S_nR}\right|^2\right), \tag{11}$$

$$\omega_3 = \max_{n=1,2,\ldots,M}\left(\left|h_{S_nD}\right|^2\right). \tag{12}$$

As in [18], the cumulative density function (CDF) of ω_i can be given by the following equation:

$$F_{\omega_i}(y) = \sum_{p=0}^{M}(-1)^p C_M^p \times e^{-py/\lambda_i}, \tag{13}$$

where λ_i is the mean of the random variable (*R*) ω_i, $i \in (1,3)$, and $C_M^p = \frac{M!}{p!(M-p)!}$.

Then, the corresponding probability density function (PDF) can be obtained by

$$f_{\omega_i}(y) = \frac{1}{\lambda_i}\sum_{p=0}^{M-1}(-1)^p C_{M-1}^{p} M \times e^{-(p+1)y/\lambda_i}. \tag{14}$$

Outage probability (OP)

From (9), the OP of a DF system can be expressed as

$$\begin{aligned} OP &= \Pr\left(\gamma_{e2e} < \gamma_{th}\right) = \Pr\left[\max\left\{\min\left(\gamma_1,\gamma_2\right),\gamma_3\right\} < \gamma_{th}\right] \\ &= \Pr\left[\min\left(\frac{(1-\rho)}{\eta\rho\left|h_{RR}\right|^2}, \frac{\eta\rho P_{S_n}\left|h_{RD}\right|^2 \max\limits_{1\le n\le M}\left|h_{S_nR}\right|^2}{N_0}\right) < \gamma_{th}\right] \times \Pr\left(\frac{P_{S_n}\max\limits_{1\le n\le M}\left|h_{S_nD}\right|^2}{N_0} < \gamma_{th}\right) \\ &= \Pr\left[\min\left(\frac{(1-\rho)}{\eta\rho\omega}, \eta\rho\gamma_0\omega_1\omega_2\right) < \gamma_{th}\right].\Pr\left(\frac{P_{S_n}\omega_3}{N_0} < \gamma_{th}\right), \end{aligned} \tag{15}$$

where we denote that $\omega = \left|h_{RR}\right|^2$, $\omega_1 = \max\limits_{1\le n\le M}\left|h_{S_nR}\right|^2$, $\omega_2 = \left|h_{RD}\right|^2$, $\omega_3 = \max\limits_{1\le n\le M}\left|h_{S_nD}\right|^2$; $\gamma_0 = \frac{P_{S_n}}{N_0}$, $\gamma_{th} = 2^{2R} - 1$ is the threshold of the proposed system, R is the source rate.

Now, we consider that

$$P_1 = \Pr\left[\min\left(\frac{(1-\rho)}{\eta\rho\omega}, \eta\rho\gamma_0\omega_1\omega_2\right) < \gamma_{th}\right] = 1 - \Pr\left[\frac{(1-\rho)}{\eta\rho\omega} \ge \gamma_{th}\right]\Pr\left(\eta\rho\gamma_0\omega_1\omega_2 \ge \gamma_{th}\right). \tag{16}$$

Let us denote that

$$P_{11} = \Pr\left[\frac{(1-\rho)}{\eta\rho\omega} \ge \gamma_{th}\right] = \Pr\left[\omega \le \frac{(1-\rho)}{\eta\rho\gamma_{th}}\right] = 1 - e^{-\frac{(1-\rho)}{\eta\rho\gamma_{th}\lambda}}, \tag{17}$$

where λ is the mean of RV ω.

$$P_{12} = \Pr\left(\eta\rho\gamma_0\omega_1\omega_2 \ge \gamma_{th}\right) = 1 - \Pr\left(\omega_2 < \frac{\gamma_{th}}{\eta\rho\gamma_0\omega_1}\right) = 1 - \int_0^{\infty} F_{\omega_2}\left(\frac{\gamma_{th}}{\eta\rho\gamma_0\omega_1} \mid \omega_1\right) f_{\omega_1}(\omega_1) d\omega_1. \tag{18}$$

By using (13), equation (18) can be reformulated as

$$P_{12} = \frac{1}{\lambda_1}\int_0^{\infty}\sum_{p=0}^{M-1}(-1)^p C_{M-1}^{p} M \times e^{-\frac{\gamma_{th}}{\eta\rho\gamma_0\omega_1\lambda_2}} \times e^{-\frac{(p+1)\omega_1}{\lambda_1}} d\omega_1 = \sum_{p=0}^{M-1}\frac{(-1)^p C_{M-1}^{p} M}{\lambda_1}\int_0^{\infty} e^{-\frac{\gamma_{th}}{\kappa\gamma_0\omega_1\lambda_2}} \times e^{-\frac{(p+1)\omega_1}{\lambda_1}} d\omega_1, \tag{19}$$

where λ_2 is the mean of RV ω_2.

Applying equation (3.324,1) from [19], equation (19) can be rewritten as

$$P_{12} = 2\sum_{p=0}^{M-1}(-1)^p C_{M-1}^{p} M \times \sqrt{\frac{\gamma_{th}}{\kappa\gamma_0\lambda_1\lambda_2}} \times K_1\left(2\sqrt{\frac{(p+1)\gamma_{th}}{\kappa\gamma_0\lambda_1\lambda_2}}\right), \tag{20}$$

where $K_v(\bullet)$ is the modified Bessel function of the second kind and v^{th} order.

Continuing, we consider that

$$P_2 = \Pr\left(\frac{P_{S_n}\omega_3}{N_0} < \gamma_{th}\right) = F_{\omega_3}\left(\frac{\gamma_{th}}{\gamma_0}\right). \tag{21}$$

From (13) and (21), we have

$$P_2 = \sum_{p=0}^{M}(-1)^p C_M^p \times e^{-\frac{p\gamma_{th}}{\gamma_0\lambda_3}}. \tag{22}$$

Substituting (18), (20), and (22) into (15), we have the OP expression as the following

$$\begin{aligned} OP &= \left[\begin{array}{l} 1-2\left(1-e^{-\frac{(1-\rho)}{\eta\rho\gamma_{th}\lambda}}\right)\times\sum_{p=0}^{M-1} \\ (-1)^p C_{M-1}^p M \times \sqrt{\frac{\gamma_{th}}{\eta\rho\gamma_0\lambda_1\lambda_2}} \times K_1\left(2\sqrt{\frac{(p+1)\gamma_{th}}{\eta\rho\gamma_0\lambda_1\lambda_2}}\right) \end{array}\right] \times \sum_{p=0}^{M}(-1)^p C_M^p \times e^{-\frac{p\gamma_{th}}{\gamma_0\lambda_3}} \\ &= \sum_{p=0}^{M}(-1)^p C_M^p \times e^{-\frac{p\gamma_{th}}{\gamma_0\lambda_3}} - 2\sum_{p=0}^{M}\sum_{l=0}^{K}(-1)^{p+l} C_M^p C_K^l (K+1)\times e^{-\frac{p\gamma_{th}}{\gamma_0\lambda_3}} \times \sqrt{\frac{\gamma_{th}}{\eta\rho\gamma_0\lambda_1\lambda_2}} \times K_1\left(2\sqrt{\frac{(l+1)\gamma_{th}}{\eta\rho\gamma_0\lambda_1\lambda_2}}\right) \\ &\quad + 2\sum_{p=0}^{M}\sum_{l=0}^{K}(-1)^{p+l} C_M^p C_K^l (K+1)\times e^{-\frac{p\gamma_{th}}{\gamma_0\lambda_3}} \times e^{-\frac{(1-\rho)}{\eta\rho\gamma_{th}\lambda}} \times \sqrt{\frac{\gamma_{th}}{\eta\rho\gamma_0\lambda_1\lambda_2}} \times K_1\left(2\sqrt{\frac{(l+1)\gamma_{th}}{\eta\rho\gamma_0\lambda_1\lambda_2}}\right). \end{aligned} \tag{23}$$

Here we denote $K = M - 1$.

Throughput

$$\tau = (1-OP)\frac{R(T/2)}{T} = (1-OP)\frac{R}{2}. \tag{24}$$

SER analysis

In this section, we obtain new expressions for the SER at the destination. We first consider the outage probability, which was obtained in [20]. Thus, SER can be defined as

$$SER = \mathrm{E}\left[\phi Q(\sqrt{2\theta\gamma_{e2e}}\right], \tag{25}$$

where $Q(t) = \frac{1}{\sqrt{2\pi}}\int_t^{\infty} e^{-x^2/2}dx$ is the Gaussian Q-function, ω and θ are constants specific for the modulation type, $(\phi,\theta) = (1,1)$ for binary phase-shift keying (BPSK), $(\phi,\theta) = (1,2)$ for quadrature phase shift keying (QPSK) and binary frequency-shift keying (BFSK) with orthogonal signaling $(\phi,\theta) = (1,0.5)$ or minimum correlation $(\phi,\theta) = (1,0.715)$. As a result, before obtaining the SER performance, the distribution function of γ_{e2e} is expected. Then, we begin rewriting the SER expression given in (25) directly in terms of the outage probability at the source by using integration, as follows:

$$SER = \frac{\phi\sqrt{\theta}}{2\sqrt{\pi}}\int_0^{\infty}\frac{e^{-\theta x}}{\sqrt{x}}F_{\gamma_{e2e}}(x)dx. \tag{26}$$

By substituting (23) into (26) and replacing $\gamma_{th} = x,$ we have

$$SER = \frac{\phi\sqrt{\theta}}{2\sqrt{\pi}} \int_0^{\infty} \frac{e^{-\theta x}}{\sqrt{x}} \left\{ \begin{array}{l} \sum_{p=0}^{M} (-1)^p C_M^p \times e^{-\frac{p\gamma_{th}}{\gamma_0\lambda_3}} - 2\sum_{p=0}^{M}\sum_{l=0}^{K} (-1)^{p+l} C_M^p C_K^l (K+1) \times e^{-\frac{p\gamma_{th}}{\gamma_0\lambda_3}} \\ \times \sqrt{\frac{\gamma_{th}}{\eta\rho\gamma_0\lambda_1\lambda_2}} \times K_1\left(2\sqrt{\frac{(l+1)\gamma_{th}}{\eta\rho\gamma_0\lambda_1\lambda_2}}\right) + 2\sum_{p=0}^{M}\sum_{l=0}^{K} \frac{(-1)^{p+l} C_M^p C_K^l (K+1)}{\times e^{-\frac{p\gamma_{th}}{\gamma_0\lambda_3}} \times e^{-\frac{(1-\rho)}{\eta\rho\gamma_{th}\lambda}}} \\ \times \sqrt{\frac{\gamma_{th}}{\eta\rho\gamma_0\lambda_1\lambda_2}} \times K_1\left(2\sqrt{\frac{(l+1)\gamma_{th}}{\eta\rho\gamma_0\lambda_1\lambda_2}}\right) \end{array} \right\} dx$$

$$= \frac{\phi\sqrt{\theta}}{2\sqrt{\pi}} \sum_{p=0}^{M} (-1)^p C_M^p \int_0^{\infty} \frac{e^{-x\left(\theta+\frac{p}{\gamma_0\lambda_3}\right)}}{\sqrt{x}} dx$$

$$- \frac{\phi\sqrt{\theta}}{\sqrt{\pi}} \sum_{p=0}^{M} \frac{\sum_{l=0}^{K} (-1)^{p+l} C_M^p C_K^l (K+1)}{\sqrt{\frac{1}{\eta\rho\gamma_0\lambda_1\lambda_2}}} \int_0^{\infty} e^{-x\left(\theta+\frac{p}{\gamma_0\lambda_3}\right)} \times K_1\left(2\sqrt{\frac{(l+1)x}{\eta\rho\gamma_0\lambda_1\lambda_2}}\right) dx$$

$$+ \frac{\phi\sqrt{\theta}}{\sqrt{\pi}} \sum_{p=0}^{M}\sum_{l=0}^{K} (-1)^{p+l} C_M^p C_K^l (K+1) \sqrt{\frac{1}{\eta\rho\gamma_0\lambda_1\lambda_2}} \int_0^{\infty} e^{-x\left(\theta+\frac{p}{\gamma_0\lambda_3}\right)} e^{\frac{(1-\rho)}{\eta\rho x\lambda}} \times K_1\left(2\sqrt{\frac{(l+1)x}{\eta\rho\gamma_0\lambda_1\lambda_2}}\right) dx. \quad (27)$$

We denote by J_1, J_2, and J_3 as shown by formulas 28–32.

$$J_1 = \frac{\phi\sqrt{\theta}}{2\sqrt{\pi}} \sum_{p=0}^{M} (-1)^p C_M^p \int_0^{\infty} \frac{e^{-x\left(\theta+\frac{p}{\gamma_0\lambda_3}\right)}}{\sqrt{x}} dx\,. \quad (28)$$

Applying equation (3.361,2) from [19], equation (28) can be rewritten as

$$J_1 = \phi\sqrt{\theta} \sum_{p=0}^{M} \frac{(-1)^p C_M^p}{\left(\theta + \frac{p}{\gamma_0\lambda_3}\right)}\,. \quad (29)$$

$$J_2 = \frac{\phi\sqrt{\theta}}{\sqrt{\pi}} \sum_{p=0}^{M}\sum_{l=0}^{K} (-1)^{p+l} C_M^p C_K^l (K+1) \sqrt{\frac{1}{\eta\rho\gamma_0\lambda_1\lambda_2}} \int_0^{\infty} e^{-x\left(\theta+\frac{p}{\gamma_0\lambda_3}\right)} \times K_1\left(2\sqrt{\frac{(l+1)x}{\eta\rho\gamma_0\lambda_1\lambda_2}}\right) dx. \quad (30)$$

Applying equation (6.614,5) from [19], equation (30) can be reformulated as

$$J_2 = \frac{\phi\sqrt{\theta}}{4} \sum_{p=0}^{M}\sum_{l=0}^{K} (-1)^{p+l} C_M^p C_K^l \frac{1}{\left(\theta + \frac{p}{\gamma_0\lambda_3}\right)^3} \times \frac{\sqrt{(l+1)}}{\eta\rho\gamma_0\lambda_1\lambda_2} \times e^{\frac{(l+1)\lambda_3}{2\eta\rho\lambda_1\lambda_2(\theta\gamma_0\lambda_3+p)}} \times \left[\begin{array}{l} K_1\left(\frac{(l+1)\lambda_3}{2\eta\rho\lambda_1\lambda_2(\theta\gamma_0\lambda_3+p)}\right) \\ -K_0\left(\frac{(l+1)\lambda_3}{2\eta\rho\lambda_1\lambda_2(\theta\gamma_0\lambda_3+p)}\right) \end{array} \right]. \quad (31)$$

$$J_3 = \frac{\phi\sqrt{\theta}}{\sqrt{\pi}} \sum_{p=0}^{M}\sum_{l=0}^{K} (-1)^{p+l} C_M^p C_K^l (K+1) \sqrt{\frac{1}{\eta\rho\gamma_0\lambda_1\lambda_2}} \int_0^{\infty} e^{-x\left(\theta+\frac{p}{\gamma_0\lambda_3}\right)} e^{\frac{(1-\rho)}{\eta\rho x\lambda}} \times K_1\left(2\sqrt{\frac{(l+1)x}{\eta\rho\gamma_0\lambda_1\lambda_2}}\right) dx. \quad (32)$$

We apply Taylor series as follows:

$$e^{-x\left(\theta+\frac{p}{\gamma_0\lambda_3}\right)}=\sum_{v=0}^{\infty}\frac{\left[-x\left(\theta+\frac{p}{\gamma_0\lambda_3}\right)\right]^v}{v!}=\sum_{v=0}^{\infty}(-1)^v\left[\left(\theta+\frac{p}{\gamma_0\lambda_3}\right)\right]^v\frac{x^v}{v!}, \tag{33}$$

$$e^{-\frac{(1-\rho)}{\eta\rho x\lambda}}=\sum_{t=0}^{\infty}\frac{\left[-\frac{(1-\rho)}{\eta\rho x\lambda}\right]^t}{t!}=\sum_{t=0}^{\infty}(-1)^t\left[\left(\frac{(1-\rho)}{\eta\rho\lambda}\right)\right]^t\frac{1}{t!x^t}. \tag{34}$$

Substituting (33) and (34) into (32), J_3 can be rewritten as

$$J_3=\frac{\phi\sqrt{\theta}}{\sqrt{\pi}}\sum_{p=0}^{M}\sum_{l=0}^{K}\sum_{v=0}^{\infty}\sum_{t=0}^{\infty}\frac{(-1)^{p+l+v+t}}{v!t!}\left[\left(\theta+\frac{p}{\gamma_0\lambda_3}\right)\right]^v\left[\left(\frac{(1-\rho)}{\eta\rho\lambda}\right)\right]^t C_M^pC_K^l(K+1)\sqrt{\frac{1}{\eta\rho\gamma_0\lambda_1\lambda_2}}$$
$$\times\int_0^{\infty}x^{v-t}\times K_1\left(2\sqrt{\frac{(l+1)x}{\eta\rho\gamma_0\lambda_1\lambda_2}}\right)dx. \tag{35}$$

Here we employ the following equation (6.561,16, from [19]):

$$\int_0^{\infty}x^{\mu}K_n\left(ax\right)dx=2^{\mu-1}a^{-\mu-1}\Gamma\left(\frac{1+\mu+n}{2}\right)\Gamma\left(\frac{1+\mu-n}{2}\right), \tag{36}$$

where $\Gamma(\bullet)$ is the gamma function.

By changing the variable $x=\sqrt{y}$, equation (36) can be reformulated as

$$\int_0^{\infty}y^{\frac{\mu-1}{2}}K_n\left(a\sqrt{y}\right)dy=2^{\mu}a^{-\mu-1}\Gamma\left(\frac{1+\mu+n}{2}\right)\Gamma\left(\frac{1+\mu-n}{2}\right). \tag{37}$$

Applying formula (37) in case $n = 1$, we obtain

$$J_3=\frac{\phi\sqrt{\theta}}{\sqrt{\pi}}\sum_{p=0}^{M}\sum_{l=0}^{K}\sum_{v=0}^{\infty}\sum_{t=0}^{\infty}\frac{(-1)^{p+l+v+t}}{v!t!}\left[\left(\theta+\frac{p}{\gamma_0\lambda_3}\right)\right]^v\left[\left(\frac{(1-\rho)}{\eta\rho\lambda}\right)\right]^t C_M^pC_K^l(K+1)\sqrt{\frac{1}{\eta\rho\gamma_0\lambda_1\lambda_2}}$$
$$\times 2^{2v-2t+1}\times\left[2\sqrt{\frac{(l+1)}{\eta\rho\gamma_0\lambda_1\lambda_2}}\right]^{-2v+2t-2}\times\Gamma\left(v-t+\frac{3}{2}\right)\times\Gamma\left(v-t+\frac{1}{2}\right). \tag{38}$$

Then J_3 can be rewritten as

$$J_3=\frac{\phi\sqrt{\theta}}{2\sqrt{\pi}}\sum_{p=0}^{M}\sum_{l=0}^{K}\sum_{v=0}^{\infty}\sum_{t=0}^{\infty}\frac{(-1)^{p+l+v+t}}{v!t!}\left[\left(\theta+\frac{p}{\gamma_0\lambda_3}\right)\right]^v\left[\left(\frac{(1-\rho)}{\lambda}\right)\right]^t C_M^pC_K^l(K+1)$$
$$\times\frac{(l+1)^{t-v-1}}{(\eta\rho)^{2t-v-1/2}\left(\gamma_0\lambda_1\lambda_2\right)^{t-v-1/2}}\times\Gamma\left(v-t+\frac{3}{2}\right)\times\Gamma\left(v-t+\frac{1}{2}\right). \tag{39}$$

Finally, the SER of the proposed system can be calculated by the following equation:

$$SER = \phi\sqrt{\theta}\sum_{p=0}^{M}\frac{(-1)^p C_M^p}{\left(\theta+\frac{p}{\gamma_0\lambda_3}\right)} - \frac{\phi\sqrt{\theta}}{4}\sum_{p=0}^{M}\sum_{l=0}^{K}(-1)^{p+l}C_M^p C_K^l \frac{1}{\left(\theta+\frac{p}{\gamma_0\lambda_3}\right)^3}\times\frac{\sqrt{(l+1)}}{\eta\rho\gamma_0\lambda_1\lambda_2}$$
$$\times e^{\frac{(l+1)\lambda_3}{2\eta\rho\lambda_1\lambda_2(\theta\gamma_0\lambda_3+p)}}\times\left[K_1\left(\frac{(l+1)\lambda_3}{2\eta\rho\lambda_1\lambda_2(\theta\gamma_0\lambda_3+p)}\right)-K_0\left(\frac{(l+1)\lambda_3}{2\eta\rho\lambda_1\lambda_2(\theta\gamma_0\lambda_3+p)}\right)\right]$$
$$+\frac{\phi\sqrt{\theta}}{2\sqrt{\pi}}\sum_{p=0}^{M}\sum_{l=0}^{K}\sum_{v=0}^{\infty}\sum_{t=0}^{\infty}\frac{(-1)^{p+l+v+t}}{v!t!}\left[\left(\theta+\frac{p}{\gamma_0\lambda_3}\right)\right]^v\left[\left(\frac{(1-\rho)}{\lambda}\right)\right]^t C_M^p C_K^l(K+1)$$
$$\times\frac{(l+1)^{t-v-1}}{(\eta\rho)^{2t-v-1/2}\left(\gamma_0\lambda_1\lambda_2\right)^{t-v-1/2}}\times\Gamma\left(v-t+\frac{3}{2}\right)\times\Gamma\left(v-t+\frac{1}{2}\right). \quad (40)$$

4. NUMERICAL RESULTS AND DISCUSSION

In this section, we investigate the multi-source in DF cooperative networks with the PSR protocol based FD energy harvesting relaying network over a Rayleigh fading channel. In this system model, the multi-source and the destination communicate with each other by both the direct link and via an intermediate helping relay [16–18]. The simulation parameters are listed in Table 1.

The influence of the power splitting factor ρ on the outage probability and throughput of the model system is shown in Fig. 3a and 3b, respectively. In the simulation process, the main parameters of the proposed system are set as follows: $M = 2$, $P_S/N_0 = 5$ dB, $R = 0.25$, 0.5, 1. The outage probability decreased and the throughput increased slightly while ρ varied from 0 to 1 (Fig. 3). Moreover, the analytical results agree well with the Monte Carlo simulation results, validating the theoretical derivations.

On the other hand, Figs 4a and 4b illustrate the influence of the energy harvesting efficiency η on the outage probability and the achievable throughput of the model system. Here, P_S/N_0 is set at 1, 3, 5 dB; $\rho = 0.5$; $M = 1$; and $R = 0.5$ bps. From the simulation, it is clear that the achievable throughput increases and the outage probability decreases slightly while η varies from 0 to 1. In this case, the figures reveal that the simulation results match tightly with the analytical expressions in Section 3.

Moreover, Fig. 5a and 5b present the effect of the number of sources M on the outage probability and the achievable throughput with $P_S/N_0 = 1$, 3, 5 dB; $R = 0.5$ bps; $\rho = 0.35$; and $\eta = 0.8$ for the proposed system. The achievable throughput increased and the outage probability decreased significantly when M increased from 1 to 10. In Fig. 5, all the analytical and the simulation results show good agreement with each other.

In the same way, the influence of the source power to noise ratio P_S/N_0 on the outage probability and the achievable throughput of the system model with $M = \{1, 3, 5\}$, $R = 0.5$ bps, $\rho = 0.35$, and $\eta = 0.8$ are illustrated in the Fig. 6a and 6b, respectively. As shown, the outage probability decreased and the system throughput increased crucially when P_S/N_0 increased from –5 to 10 dB. In particular, the simulation lines wholly match with the analytical lines in the above figures.

Finally, SER of the proposed system versus M and the ratio P_S/N_0 are presented in Fig. 7 and Fig. 8, respectively. In these figures, the simulation results match tightly with analytical expressions in Section 3.

Table 1. Simulation parameters

Name	Symbol	Value
Energy harvesting efficiency	η	0.8
Mean of $\lvert h_{SR}\rvert^2$	λ_1	0.5
Mean of $\lvert h_{RD}\rvert^2$	λ_2	0.5
Mean of $\lvert h_{SD}\rvert^2$	λ_3	0.5
Mean of $\lvert h_{RR}\rvert^2$	λ	0.5
SNR threshold	γ_{th}	1
Source power to noise ratio	P_S/N_0	–5 to 10 dB
Source rate	R	0.5 (bit/s)/Hz

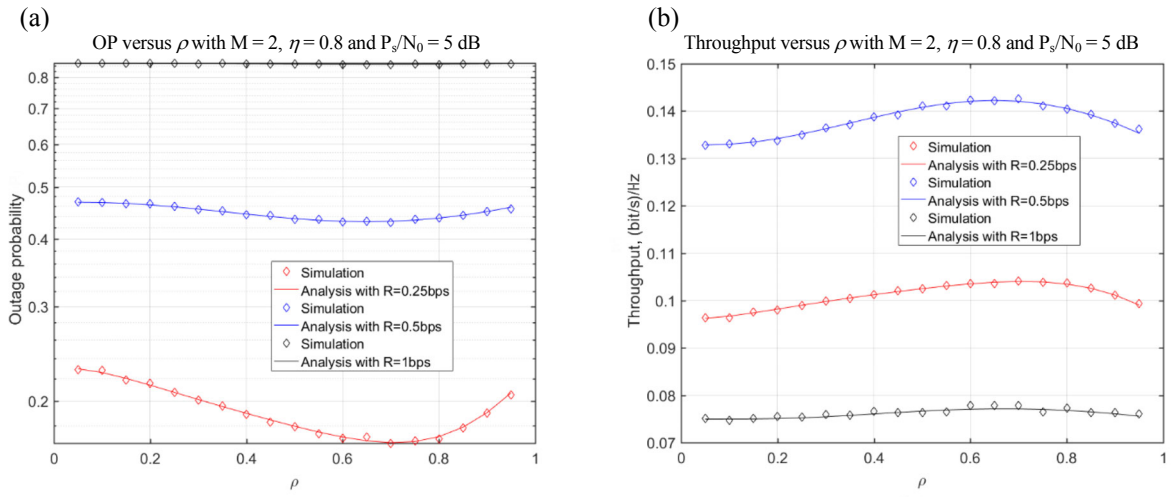

Fig. 3. Outage probability (a) and achievable throughput (b) versus the power splitting factor ρ.

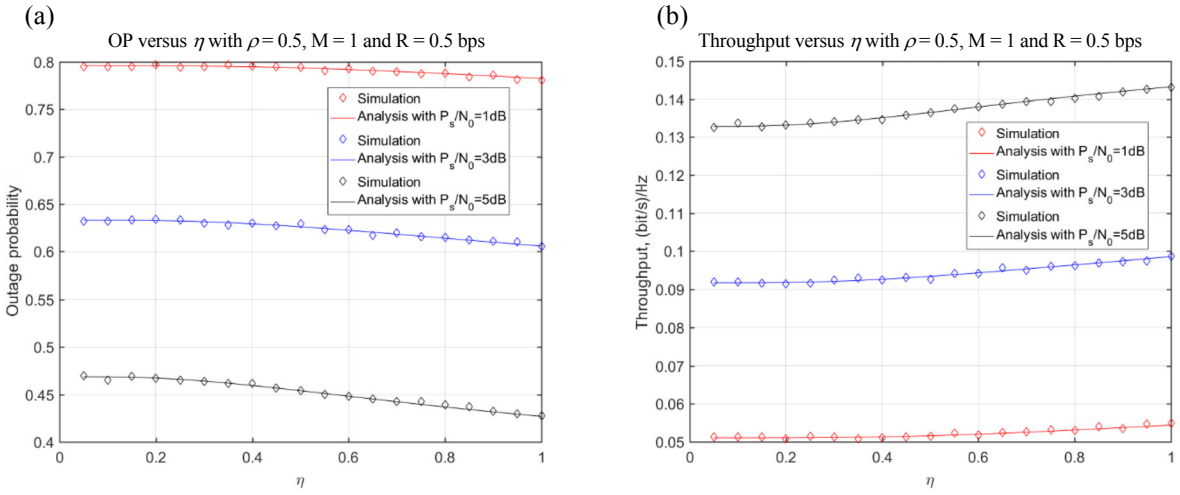

Fig. 4. Outage probability (a) and achievable throughput (b) versus the energy harvesting efficiency η.

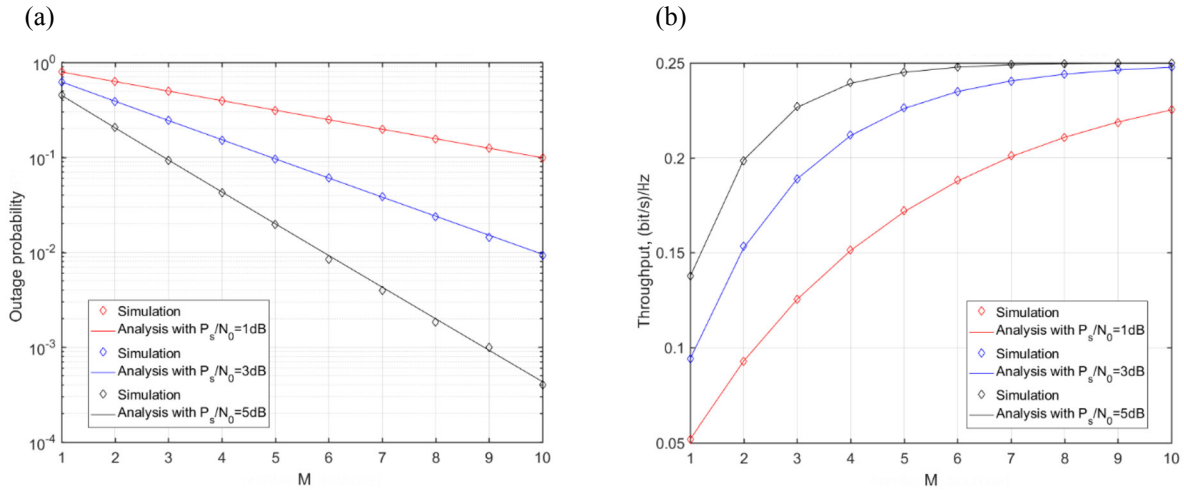

Fig. 5. Outage probability (a) and achievable throughput (b) versus the number of sources M.

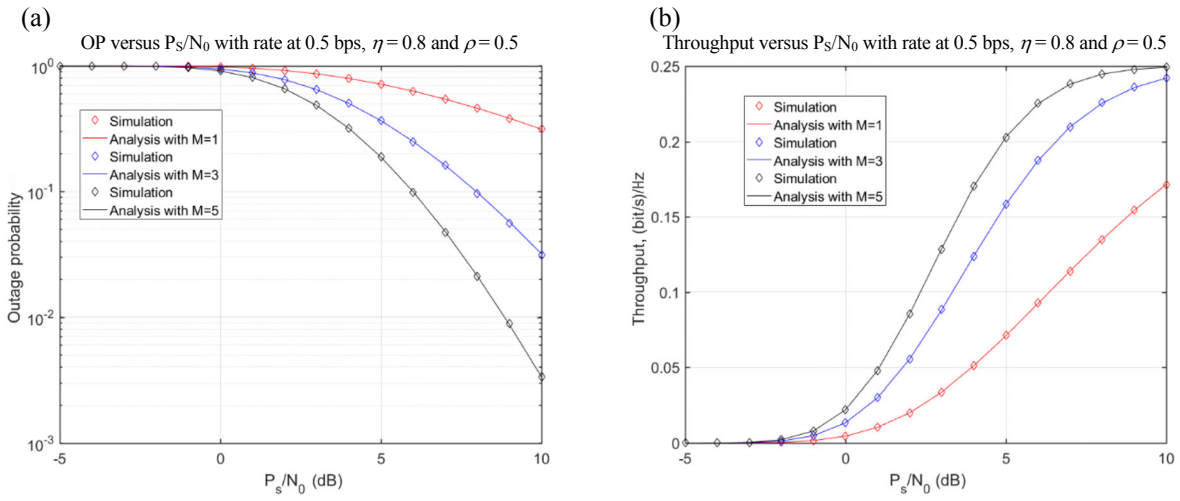

Fig. 6. Outage probability (a) and achievable throughput (b) versus the source power to noise ratio P_S/N_0.

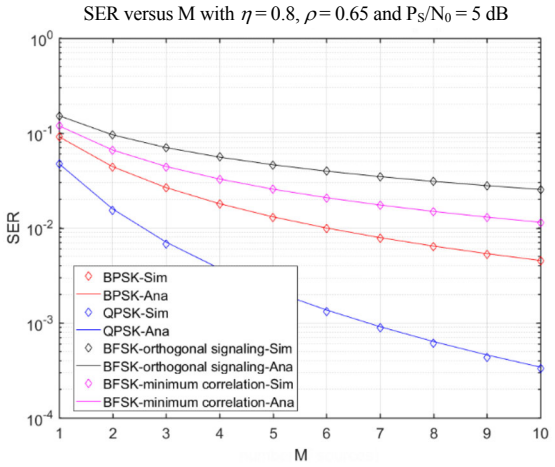

Fig. 7. SER versus the number of sources M.

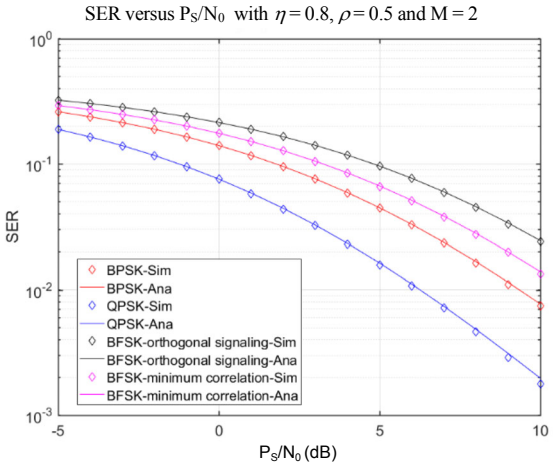

Fig. 8. SER versus the source power to noise ratio P_S/N_0.

5. CONCLUSION

In this paper, we investigated the multi-source in decode-and-forward (DF) cooperative networks with the power splitting (PSR) protocol based full-duplex (FD) energy harvesting relaying network over a Rayleigh fading channel. We presented the source selection for improving the system performance of the model system. Then, the closed-form expression of the outage probability and the symbol error ratio (SER) were derived. Finally, the Monte Carlo simulation was used for validating the analytical expressions in connection with all main possible system parameters. From the research results, we can see that the analytical and simulation results matched well with each other. The results can be proposed as a novel approach for the communication network in the near future.

ACKNOWLEDGEMENTS

This work was supported by the grant SGS registration No. SP2018/59 conducted at VSB Technical University of Ostrava, Czech Republic, and partly by The Ministry of Education, Youth and Sports from the Large Infrastructures for Research, Experimental Development, and Innovations project registration No. LM2015070. The publication costs of this article were partially covered by the Estonian Academy of Sciences.

REFERENCES

1. Niyato, D., Kim, D. I., Maso, M., and Han, Z. Wireless powered communication networks: research directions and technological approaches. *IEEE Wireless Commun.*, 2017, **24**, 88–97.
2. Yu, H., Lee, H., and Jeon, H. What is 5G? Emerging 5G mobile services and network requirements. *Sustainability*, 2017, **9**, 1848.
3. Salari, S., Kim, I-M., Kim, D. I., and Chan, F. Joint EH time allocation and distributed beamforming in interference-limited two-way networks with EH-based relays. *IEEE Trans. Wireless Commun.*, 2017, **16**, 6395–6408.
4. Jameel, F., Wyne, S., and Ding, Z. Secure communications in three-step two-way energy harvesting DF relaying. *IEEE Commun. Lett.*, 2018, **22**, 308–311.
5. Peng, C., Li, F., and Liu, H. Optimal power splitting in two-way decode-and-forward relay networks. *IEEE Commun. Lett.*, 2017, **21**, 2009–2012.
6. Singh, S., Modem, S., and Prakriya, S. Optimization of cognitive two-way networks with energy harvesting relays. *IEEE Commun. Lett.*, 2017, **21**, 1381–1384.
7. Cai, G., Fang, Y., Han, G., Xu, J., and Chen, G. Design and analysis of relay-selection strategies for two-way relay network-coded DCSK systems. *IEEE Trans. Vehicular Technol.*, 2018, **67**, 1258–1271.
8. Perera, T. D. P., Jayakody, D., N. K., Sharma, S. K., Chatzinotas, S., and Li, J. Simultaneous wireless information and power transfer (SWIPT): recent advances and future challenges. *IEEE Commun. Surv. Tutor.*, 2018, **20**, 264–302.
9. Nasir, A. A., Zhou, X., Durrani, S., and Kennedy, R. A. Relaying protocols for wireless energy harvesting and information processing. *IEEE Trans. Wireless Commun.*, 2013, **12**, 3622–3636.
10. Bhatnagar, M. R. On the capacity of decode-and-forward relaying over Rician fading channels. *IEEE Commun. Lett.*, 2013, **17**, 1100–1103.
11. Ju, H. and Zhang, R. Throughput maximization in wireless powered communication networks. In *2013 IEEE Global Communications Conference (GLOBECOM)*. IEEE, 2013.
12. Huang, K. and Vincent, L. K. N. Enabling wireless power transfer in cellular networks: architecture, modeling and deployment. *IEEE Trans. Wireless Commun.*, 2014, **13**, 902–912.
13. Okandeji, A. A., Khandaker, M. R. A., and Wong, K-K. Two-way beamforming optimization for full-duplex SWIPT systems. In *Proceedings of the 24th European Signal Processing Conference (EUSIPCO)*. IEEE, Budapest, Hungary, 2016.
14. Okandeji, A. A., Khandaker, M. R. A., Wong, K-K., and Zheng, Z. Joint transmit power and relay two-way beamforming optimization for energy-harvesting full-duplex communications. In *2016 IEEE Globecom Workshops (GC Wkshps)*. IEEE, Washington, DC, 2016.
15. Hu, Y., Zhu, Y., and Schmeink, A. Simultaneous wireless information and power transfer in relay networks with finite blocklength codes. In *23rd Asia-Pacific Conference on Communications (APCC)*. IEEE, 2017.
16. Nguyen, T. N., Minh, T. H. Q., Tran, P. T., and Voznak, M. Energy harvesting over Rician fading channel: a performance analysis for half-duplex bidirectional sensor networks under hardware impairments. *Sensors*, 2018, **18**, 1781.
17. Tan, N. N., Minh, T. H. Q., Tran, P. T., and Voznak, M. Adaptive energy harvesting relaying protocol for two-way half duplex system network over Rician fading channel. *Wireless Comm. Mobile Comp.*, **2018**, Article ID 7693016.
18. Nguyen, T. N., Duy, T. T., Luu, G-T., Tran, P. T., and Voznak, M. Energy harvesting-based spectrum access with incremental cooperation, relay selection and hardware noises. *Radioengineering*, 2017, **26**, 240–250.
19. Gradshteyn, I. S. and Ryzhik, I. M. *Table of Integrals, Series, and Products*. Elsevier, 2015.
20. McKay, M. R., Grant, A. J., and Collings, I. B. Performance analysis of MIMO-MRC in double-correlated Rayleigh environments. *IEEE Trans. Commun.*, 2007, **55**, 497–507.

PSR-protokollil põhinevad täisdupleksenergia noppega, mitme allika ja Rayleigh' sumbekanaliga DF-kooperatiivsed võrgud: toimimise analüüs

Tan N. Nguyen, Minh Tran, Duy-Hung Ha, Tran Thanh Trang ja Miroslav Voznak

Tingituna ülisuurest energiatarbe kasvust, mis tuleneb omavahel võrguühenduses olevate seadmete arvu plahvatuslikust kasvust, on ülioluline uurida alternatiivseid traadita info ja võimsuse ülekande tehnikaid. Uuringud ei ole tähtsad mitte ainult teoreetilisi tulemusi silmas pidades, vaid ka seepärast, et kokku hoida võrkude opereerimiskulutusi ja tagada jätkusuutlik traadita side areng. Antud artiklis on uuritud mitme allikaga dekodeerimise ja edastamise kooperatiivseid võrke võimsuse hakkimise protokollil põhineva täisdupleksenergia noppega vahetusvõrkudes üle Rayleigh' sumbekanalite. Nimetatud süsteemis suhtlevad mitu allikat ja sihtport teineteisega mõlemas suunas otse ning ka üle abistava vaherelee. Esiteks on uuritud allikate valikuid tagamaks süsteemi paremat sooritust. Uuringust on tuletatud valem katkestuse tõenäosuse ja sümboli vea vahekorra määramiseks. Lõpuks on kasutatud Monte Carlo simulatsioone tõestamaks saadud analüütilise valemi kehtivust, arvestades kõiki olulisi süsteemi parameetreid. Uurimus näitab analüütilisest valemist ja numbrilistest simulatsioonidest saadud tulemuste omavahelist kokkulangevust.